Electrocapillary Wave Studies of Oligomeric Ethers: Poly(dimethylsiloxane) and Poly(ethylene glycol)

Randy J. Skarlupka,† Yongsok Seo,*,‡ and Hyuk Yu*

Department of Chemistry, University of Wisconsin, Madison, Wisconsin 53706

Received July 23, 1996; Revised Manuscript Received December 9, 1996[⊗]

ABSTRACT: With the aid of a technique that induces electric field-generated capillary waves on polymeric liquid surfaces and the resulting wave propagation characteristics detected by an optical diffraction method, we examined the surface tension and steady shear viscosity of low molecular weight poly(dimethylsiloxane) (PDMS) and poly(ethylene glycol) (PEG) at different temperatures. The surface tension values are in quite good agreement with those reported in the literature, whereas the shear viscosity values are not as accurate, though they agree within 7% with those determined by a capillary viscometer. The temperature dependences of the surface tensions of both are in agreement with the literature. On the other hand, they differ in their molecular weight dependences, though PDMS shows a small difference due to its relatively small molecular weight, but the PEG slope was in good agreement in spite of its low molecular weight due to its hydrogen bonding. PDMS and PEG show different mode behaviors at high frequency and low temperature because of the overdamped mode appearance for PEG.

Introduction

Structure and properties of polymeric surfaces and interfaces are of crucial importance to a broad range of polymer technologies.[1−4] A singular parameter that characterizes polymer surfaces is the surface tension. Since the early 1960s, interfacial and surface tensions of polymeric systems have been extensively accumulated to a vast literature, some of which is well summarized in a monograph by Wu.[5] Among various experimental methods adopted for surface tension measurements on polymeric liquids are the maximum bubble pressure method, the sessile bubble technique, the ring method, the Wilhelmy plate procedure, and the pendant drop technique. Another set of noninvasive methods relies on optical techniques.[6] A variety of such techniques has been developed or implemented in recent years, and much has been learned anew relative to the static and dynamic properties of liquid surfaces and interfaces.[6] Among them are the techniques of inelastic light scattering by spontaneous surface phonons[7] (surface light scattering, SLS, for short), much like that of Brillouin scattering in bulk liquid,[8−10] and by excited surface phonons induced by electric, mechanic, or magnetic capillarity.[11] Both provide dynamic information of the liquid surfaces, whereas they differ principally in two respects. First, the frequency range of interest is set by the scattering angle range, i.e., momentum transfer, in SLS while it is set by the imposed frequency range of external field in the latter method; the one relying on electrocapillarity detected by optical diffraction is called electrocapillary wave diffraction, ECWD for short, and this is the one we use in this study. Second, the wave damping in SLS is provided in the temporal domain, whereas that in ECWD is in the spatial domain; hence there exists some difference in the detected frequency ranges in the two methods. Both of these techniques have been used in this laboratory to investigate the surface or interfacial properties of bulk liquids of low molecular weight or dynamic viscoelastic properties of the polymeric monolayer.[12−16] Because of viscosity of bulk liquids or concentrated solutions of polymers exceeding a few poises, these techniques however are seldom applied to examine the surface properties of such systems.

Besides the different detecting frequency range[16] (less than 5 kHz), ECWD has an advantage over the surface light scattering technique; while SLS relies on thermally induced spontaneous capillary waves at both liquid/liquid and air/liquid interfaces, ECWD takes an alternative approach in that capillary waves of desired frequency are externally generated through an AC electrical field. In the propagating wave regime, the SLS technique has a fairly low viscosity limit (≈5 cP). On the other hand, the theoretical upper limit of viscosity for ECWD in the same regime is several poises.[16]

Here, we report our examination of the liquids of oligomeric ethers, siloxanes, and ethylene glycols, with respect to their surface tensions and steady shear viscosities at different temperatures by means of the ECWD. The main focus is to show that the method gives rise to a consistent set of results as those by the more conventional methods and in the literature.

Table 1. Characteristics of Oligomer Samples

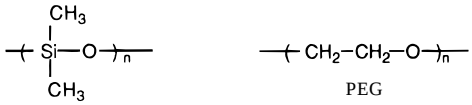

PDMS PEG

polymer	MW (g/mol)	DP[c]	M_w/M_n
PDMS	1250	17	1.46
PEG	350	8	2.15

[a] Degree of polymerization.

Experimental Methods

Materials. Commercially available samples of two oligomers having relatively low molecular weight were used in this study. The first one is poly(dimethylsiloxane), PDMS (Petrarch Systems, PS039). The second is poly(ethylene glycol), PEG (Scientific Polymer Products, #496). The sample characteristics are listed in Table 1. These two polymer

† Permanent address: Polymer Composites Inc., 4610 Theuere Blvd, P.O. Box 30010, Winona, MN 55987-1010.

‡ Permanent address: Polymer Processing Laboratory, KIST, P.O. Box 131, Cheongryang, Seoul, Korea.

⊗ Abstract published in *Advance ACS Abstracts,* January 15, 1997.

S0024-9297(96)01095-9 CCC: $14.00

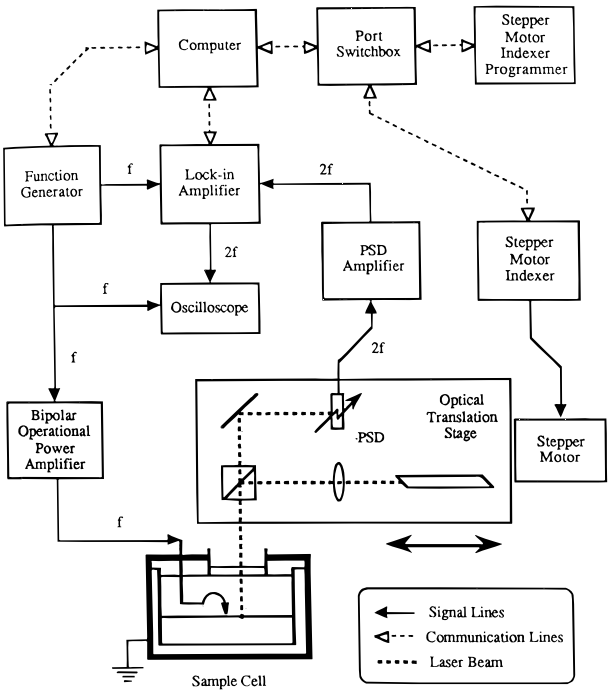

Figure 1. Block diagram of the ECWD apparatus.

systems were chosen because they are in the liquid state at room temperature and their viscosities are within the limits of our detection capability with ECWD. The choice of the two is based on the fact that the surface tension of PDMS shows a weak dependence on molecular weight whereas that of PEG is found to be independent of molecular weight even in the oligomeric range.[5] The difference is commonly attributed to strong hydrogen bonding (between the terminal hydroxyl groups) of PEG, which effectively makes the oligomers behave as though having a very large molecular weight; hence PDMS and PEG show different characteristic surface wave behaviors. The samples were purified by mixing with activated carbon (DarcoG60 from Aldrich) to remove any surface active impurities and filtering through 0.5 μm filters, and the procedure was repeated twice for each sample.

All glassware and the Teflon trough (see below) were cleaned with a sulfuric acid−Nochromix (Godax Labs, NY) solution and rinsed thoroughly with deionized water processed through a Milli-Q ion exchange and filtration system (Millipore), which is fed by the house distilled water.

Electrocapillary Wave Diffraction Method. A block diagram of the experimental setup is shown in Figure 1, a description of which was reported earlier.[16] Briefly, electrocapillary waves are excited by applying an intense local AC electric field over a small area on the surface through a source needle positioned within about 100 μm from the interface. Others use a razor blade rather than a needle.[17] Razor blades can generate a capillary wave having larger amplitudes. However, as shown in our previous studies, use of a needle rather than a razor blade has several advantages even though the waves generated damp faster than those by the razor blade. They are as follows: (1) We can avoid a possible edge effect of the blade, (2) we can prevent dealing with nonplanarity in the detection of generated waves in cases where the blade axis is not perfectly parallel with the interface, and (3) we can eliminate errors prone to determinations of the displacement distance r from the source axis by placing the laser beam scanning axis off-perpendicular to the razor blade line. By the application of an AC electric field, because of a difference in dielectric permittivity across the interface, a circular ripple with a spatial wavelength on the order of 0.3−3 mm and an amplitude-to-wavelength ratio on the order of 10^{-3}−10^{-5} are generated, whereby we have a situation where the measurements are macroscopic in character, as is required in any viscoelastic measurement.[18]

The modeling function of the damped circular wave profile is represented by the zeroth-order circular Bessel function,[19,20]

$$J_0(r) = \sum_{n=0}^{\infty} \frac{(-1)^n (k_o r)^{2n}}{n!\,\Gamma(n+1)} \tag{1}$$

where k_o is the capillary wave vector, r is the radial distance from the center of the wave, and $\Gamma(n+1)$ is the gamma function, which can be approximated by a Hankel function (exponential decay):

$$H_0(x) = \left(\frac{2}{\pi k_o r}\right)^{-1/2} \cos\left(k_o r - \frac{\pi}{4}\right) \tag{2}$$

under the condition of a large distance away from the source point. The errors involved in the amplitude calculation by the approximation have been evaluated to be less than 0.05% if the distance is larger than the first three wave peaks and to be less than 0.7% even if the distance is at the first valley of the wave. The values of measured damping coefficients and wavelengths of capillary waves were in good agreement with those obtained by plane waves.[20] Displayed in Figure 2 is a view of the 3-D surface representing the waves produced by the ECWD technique, though the amplitude-to-wavelength ratio is highly exaggerated. The modeling function represents the wave motion of ideal liquids, i.e., liquids with zero viscosity. Since we are using real viscous liquids, the wave motion we encounter is always accompanied by dissipation of mechanical energy into heat. If we take into consideration this energy dissipation, then we obtain the wave profile[16,20,21] as

$$\Psi(r,t) = \frac{\Psi_O}{\sqrt{r}}\, e^{-\beta r} \cos(k_o r + 2\omega t) \tag{3}$$

where β is the spatial-damping constant. Hence the phase difference $k_o r$ and wave-damping coefficient are proportional to r and $\ln[r^{1/2}\Psi(r,t)]$, respectively. By scanning along a given radial axis from the tip of the needle, sets of the phase difference and amplitude as functions of r are obtained. By plotting the phase difference and natural logarithm of the corrected amplitude, $\ln[r^{1/2}\Psi(r,t)]$, one obtains straight lines whose slopes are exactly k_o and β, respectively. Examples of such plots are shown in Figure 3 for the test system of PDMS. The expected linearities of the phase difference and corrected amplitude versus the radial distance r are well borne out for each of the frequencies. However, at high frequency (>2 kHz), deviation from the linearities becomes apparent at a short radial distance from the source point. As will be discussed later, this is attributed to a different mode behavior.

The spatial wave vector k_o and the corresponding wave-damping coefficient β for the capillary waves thus determined are then used in the following dispersion equation for surface waves to deduce the surface tension γ or interfacial tension σ and the bulk shear viscosity of one fluid phase η:

$$[\epsilon^* k^{*2}/\omega + i\eta(k^* + m) + i\eta'(k^* + m')][i\eta(k^* + m) + i\eta'(k^* + m') + \sigma^* k^{*2}/\omega + g(\rho - \rho')/\omega - \omega(\rho + \rho')/k^*] + [\eta(k^* - m) - \eta'(k^* - m')]^2 = 0 \tag{4}$$

where $k^* = k_o + i\beta$, $m \equiv [k^{*2} + i\omega\rho/\eta]^{1/2}$, $m' \equiv [k^{*2} + i\omega\rho'/\eta']^{1/2}$, ω is angular frequency, g is the gravitational constant, η and η' are the shear viscosities of air (or upper phase) and subphase, respectively, ρ and ρ' are the corresponding densities, $\epsilon^* \equiv \epsilon + i\omega\kappa$, where ϵ is the dynamic surface dilational elasticity and κ is the corresponding viscosity, and $\sigma^* \equiv \sigma + i\omega\mu$, where σ is the dynamic surface tension and μ is the transverse viscosity. The dilational storage and loss components, ϵ and κ, of the complex modulus ϵ^* are calculated from experimentally determined values of k_o and β at fixed ω by assuming that μ (the transverse viscosity) is zero,[16,18] so that σ^* is equal to static surface tension σ, which is in turn accessible experimentally by the conventional static techniques such as the Wilhelmy plate method. The instrument was

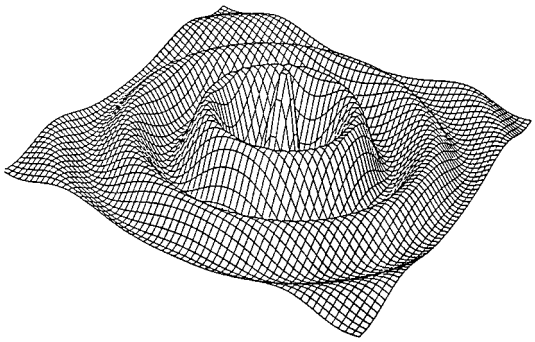

Figure 2. Representation of the circular waves produced by the ECWD technique (not to scale for the amplitude-to-wavelength ratio, which is of the order of 1/1000).

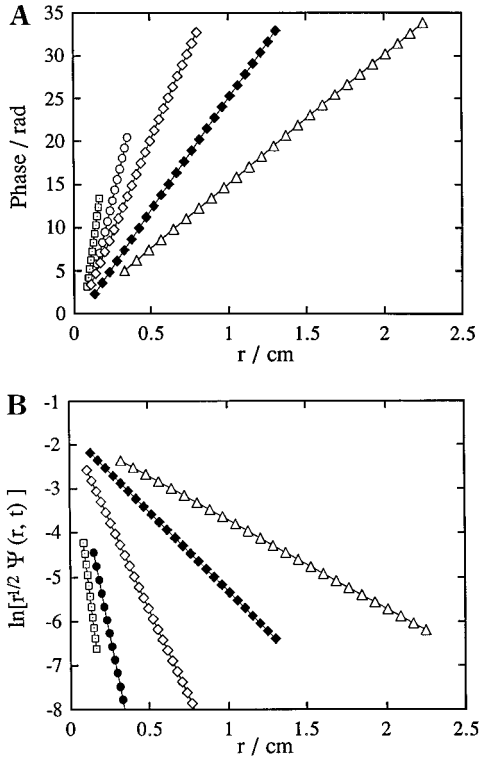

Figure 3. (A) Plots of phase angle difference between the excitation field and capillary wave against radial distance r from the field source point, the needle tip, at different excitation field frequencies f: (△) 50, (◆) 100, (◇) 200, (○) 500, and (⊡) 1000 Hz. (B) Plots of natural logarithm of the corrected amplitude, $\ln[r^{1/2}\Psi(r)]$, against r for the test system of PDMS, at different excitation field frequencies f: (△) 50, (◆) 100, (◇) 200, (●) 500, and (⊡) 1000 Hz. The spatial wave vector k_o and damping coefficient β are deduced from the slopes of these lines.

calibrated with the surface tensions of water and toluene and the interfacial tension of heptane/water under the assumption that ϵ^* is equal to zero for pure liquids.[16]

Results and Discussion

At the outset, we demonstrate some limiting behaviors of the capillary waves. The frequency dependences of the wave vector and damping constant at three different temperatures for the air/PDMS system are shown in Figure 4, where both are in a double-logarithmic scale for showing simple power laws governing the dependences even though they are limited in a range of 2 logarithmic decades in the independent variable, i.e., frequency, and 1 decade in the dependent variables. Since there is no spread monolayer and apparently no specific adsorption from the bulk phase

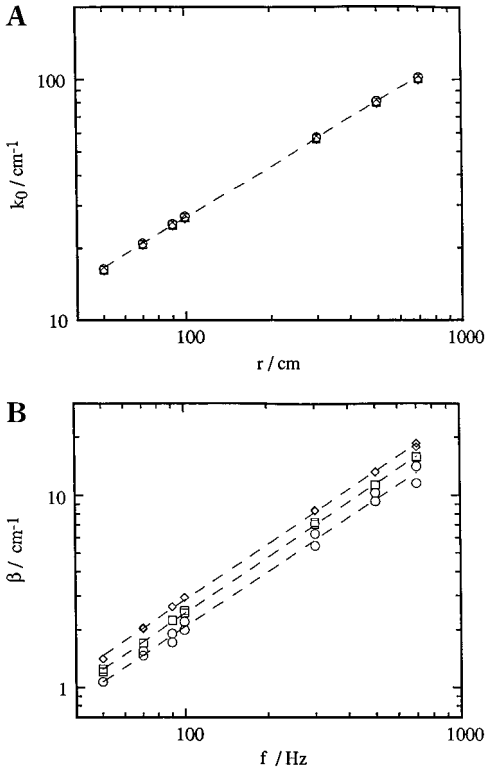

Figure 4. (A) Deduced spatial wave vector k_o as a function of frequency at (◇) 40 °C, (□) 55 °C, and (○) 70 °C. The slope of the dashed line is 0.68. (B) Deduced damping constant as a function of frequency at the same three temperatures as in panel A.

at the surface, surface viscoelastic parameters can be neglected, $\epsilon = \kappa = 0$, and further when the shear viscosity of the subphase is small, eq 4 leads to

$$\omega^2 = \frac{\gamma k^{*3}}{\rho} + gk + \frac{4i\omega\eta k^{*2}}{\rho} \tag{5}$$

which, for $\eta = 0$, reduces to the classical Kelvin equation for surface waves.[22] In our frequency range, the effect of the gravity wave is negligible, so that $k_o \propto \omega^{2/3}$, whereby the power law should emerge in a double-logarithmic plot in Figure 4A, provided that the viscosity of PDMS is not large enough to affect the capillary wave propagation behavior as manifested by the Kelvin and Stokes limiting behaviors. By allowing η to be nonzero, and setting $k^* = k_o + i\beta$, one finds that k_o is related to ω through the Kelvin equation and that

$$\beta = \frac{4k_o^3\eta}{3\rho\omega} \tag{6}$$

which has been derived by Stokes.[23] Hence, if $k_o \propto \omega^{2/3}$, then $\beta \propto \omega$. Thus, it is displayed in Figure 4B the observed frequency dependence of the wave-damping constant of PDMS. When $k_o \propto \omega^{2/3}$, since the effect of viscosity is small, the wave vector does not show any noticeable variation with temperature in our experimental range. On the other hand, the viscosity variation with temperature clearly affects the damping constant. The values of surface tension and viscosity for PDMS, thus deduced for different temperatures over the frequency ranges examined, are collected in Table 2. As in the case of the simple liquids, we do not obtain any indication for frequency dependences of σ and η over the range examined. In short, what we deduce from

Table 2. Summary of ECWD Results in the Surface Tension and Viscosity of PDMS and PEG at Different Temperatures[a]

	σ (dyne/cm)			η (cP)		
f (Hz)	40 °C	55 °C	70 °C	40 °C	55 °C	70 °C
			PDMS			
50	18.85 ± 0.01	17.96 ± 0.04	17.10 ± 0.01	8.01 ± 0.02	6.55 ± 0.16	5.35 ± 0.02
70	18.88 ± 0.01	17.95 ± 0.01	17.00 ± 0.02	8.25 ± 0.12	6.48 ± 0.03	5.25 ± 0.21
90	18.49 ± 0.02	17.63 ± 0.02	16.65 ± 0.01	8.02 ± 0.02	6.47 ± 0.05	4.75 ± 0.25
100	18.88 ± 0.01	17.90 ± 0.01	16.95 ± 0.05	8.30 ± 0.03	6.49 ± 0.18	5.15 ± 0.22
300	18.75 ± 001	17.85 ± 0.25	16.90 ± 0.15	7.85 ± 0.04	6.48 ± 0.11	4.80 ± 0.28
500	18.75 ± 0.12	17.75 ± 0.01	16.85 ± 0.01	7.62 ± 0.03	6.18 ± 0.03	4.85 ± 0.15
700	18.75 ± 0.20	17.65 ± 0.04	16.8 ± 0.03	7.5 ± 0.18	6.02 ± 0.13	4.95 ± 0.30
avg	18.76 ± 0.14	17.81 ± 0.13	16.89 ± 0.13	7.93 ± 0.3	6.38 ± 0.20	4.95 ± 0.30
capillary viscometry				7.6 ± 0.1	6.0 ± 0.1	4.8 ± 0.1
			PEG			
50	39.70 ± 0.20	38.25 ± 0.03	37.05 ± 0.01	20.10 ± 0.51	13.30 ± 0.01	9.41 ± 0.12
70	39.81 ± 0.05	38.41 ± 0.05	37.02 ± 0.21	21.20 ± 0.72	13.35 ± 0.02	9.32 ± 0.26
90	39.25 ± 0.15	39.95 ± 0.08	36.70 ± 0.23	20.01 ± 0.22	13.25 ± 0.15	9.42 ± 0.18
100	39.75 ± 0.12	38.35 ± 0.06	37.15 ± 0.04	20.62 ± 0.25	13.30 ± 0.10	9.37 ± 0.21
300	40.13 ± 0.15	38.35 ± 0.21	37.22 ± 0.26	20.30 ± 0.31	12.95 ± 0.05	9.10 ± 0.16
500	40.60 ± 1.55	38.40 ± 0.15	37.25 ± 1.06	21.27 ± 0.88	12.60 ± 0.12	9.04 ± 0.05
700	40.35 ± 0.15	39.20 ± 0.20	37.10 ± 0.56	20.02 ± 0.21	12.72 ± 0.08	8.96 ± 0.02
900	39.65 ± 0.16	38.75 ± 0.05	37.23 ± 0.60	19.12 ± 0.05	11.02 ± 1.12	8.90 ± 0.02
avg	39.90 ± 0.43	38.45 ± 0.37	37.09 ± 0.18	20.31 ± 0.68	12.81 ± 0.78	9.19 ± 0.21
capillary viscometry				18.7 ± 0.2	12.0 ± 0.1	8.6 ± 0.1

[a] Errors on the individual entries stand for one standard deviation, whereas the errors on the average values are one standard deviation of the mean values.

Table 3. Temperature Dependence of Surface Tension and Viscosity[a]

	$d\sigma/dT$[b]	$d\eta/dT$[c] (cP/K)			
polymer	((mN/m)/K)	ECWD	viscometry	WLF	Arrhenius
PDMS	−0.065	−0.099	−0.093	−0.098	−0.098
PEG	−0.093	−0.371	−0.371	−0.371	−0.376

[a] Regression errors are estimated to be about 1 % for surface tension and 1.5% for viscosity. [b] Literature values are −0.056 and −0.098 (mN/m)/K for PDMS and PEG, respectively. [c] In the experimental temperature range (40−70 °C).

ECWD are the static limits of surface tension and shear viscosity of a PDMS oligomeric liquid.

Comparison with the surface tension values in the literature confirms that the static limit deduced from ECWD is in accord with those obtained by conventional means.[5] The temperature coefficient for the surface tension is determined as −0.065 ± 0.005 (mN/m)/K, which is close to the literature value of −0.056.[5] The slight difference is attributed to the lower molecular weight of our polymer sample. The PDMS sample used here has a polydispersity (M_w/M_n) of 1.46. Surface tension data for mixtures of PDMS oligomers suggest that the lower molecular weight species are concentrated at the surface.[24] The steady shear viscosity of the sample was also measured using a Cannon-Fenske capillary viscometer. These values are included in Table 3 for comparison. It is apparent that we can deduce the visocity to within 6% of that by viscometry of PDMS. Although a span of 30 °C is rather narrow in the temperature interval to reach a conclusive point, we can at least compare our results to those predicted by the WLF equation:

$$\log \frac{\eta(T)}{\eta(T_o)} = -\frac{c_1^o(T - T_o)}{c_2^o + T - T_o} \tag{7}$$

with $c_1^o = 1.90$, $c_2^o = 222$ K, and $T_o = 303$ K for PDMS.[25] They are found to be in accord. Alternatively, we can also obtain the temperature dependence, $d\eta/dT$, by means of an Arrhenius plot since our observing temperature of 40−70 °C is so far above the glass transition of PDMS, 150 K, wherein the WLF behavior becomes indistinguishable from the Arrhenius dependence. This is listed in Table 3 together with $d\sigma/dT$.

An interesting phenomenon displayed by the PDMS is the presence of surface waves with the fundamental frequency as that of the applied potential. As was discussed in our previous report,[16] the only surface waves we expect are those of the second harmonic, twice that of the applied potential. On the other hand, we had an indication that a capilary wave with the fundamental frequency of applied potential contaminated the second harmonic wave. Thus, we set the lock-on amplifier to the fundamental frequency as well as to the second harmonic to detect the waves. Resulting behaviors are displayed in Figure 5A where both the '1f' and '2f' characters are shown on a log−log plot of wave amplitude as a function of applied voltage. As was discussed earlier by Sohl and Miyano,[26] if the applied potential ϕ contains both a DC component (V_d) with the intended AC component (V_a) at an angular frequency ω, then the input potential is $\phi = V_d + V_a \cos \omega t$, and since the force F acting on the surface is proportional to the square of the applied voltage, the force is in the form:

$$F \sim V_d^2 + (1/2)V_a^2 + 2V_dV_a \cos \omega t + V_a^2(\cos 2\omega t)/2 \tag{8}$$

which shows that waves at both the fundamental and the second harmonic are present and that for certain values V_d of V_a, the waves will be comparable in amplitude. We speculate that the origin of our '1f' signal is not necessarily attributed to such a DC component of the applied potential but rather to the inherent structure of PDMS, which is known to have a helical conformation in bulk[27] and on the air/water interface,[28] resulting in a net dipole moment at the surface. If the surface contains permanent electric dipoles, then an

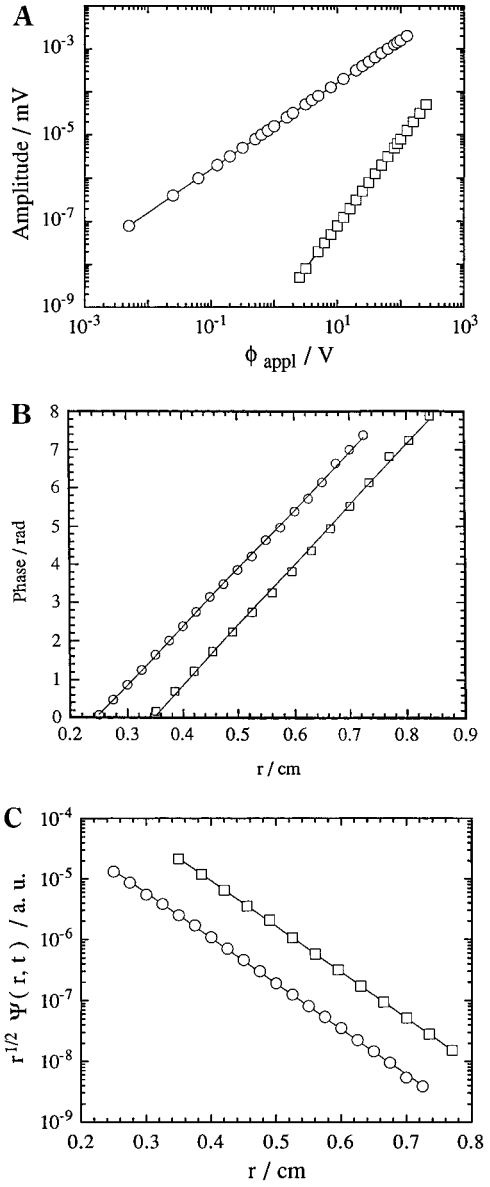

Figure 5. (A) Comparison of the wave amplitude dependence on applied voltage. Both fundamental (○) and second harmonic (□) waves are produced in the air/PDMS system (f = 50 Hz, T = 22 °C). (B) Comparison of the wave vector obtained from the '1f (○) and '2f (□) waves for the same surface frequency. The slope values of the lines are 15.24 for '1f wave and 15.73 for '2f wave. (C) Comparison of the damping constant obtained from the '1f (○) and '2f (□) waves for the same surface frequency. The slope values of the lines are −7.44 for '1f wave and −7.50 for '2f wave.

additional force proportional to the field gradient will emerge in the presence of an electric field.[29] Provided such a force exists, the wave amplitude for the '1f waves should be proportional to the applied voltage. This is in contrast to the '2f waves in which the wave amplitude is proportional to the squares of the applied voltage. Figure 5B,C compares the wave vector and damping constant obtained from the '1f and '2f wave vectors for the same surface frequency. It becomes quite apparent that the capillary wave properties are, for the most part, unaffected by the 1f mode generation.

We now turn to the second polymer system, that being PEG. Characteristics for the polymer are listed in Table 1. Surface tension and viscosity data for PEG as a function of frequency at three different temperatures are all collected in Table 2. Once again, we see no

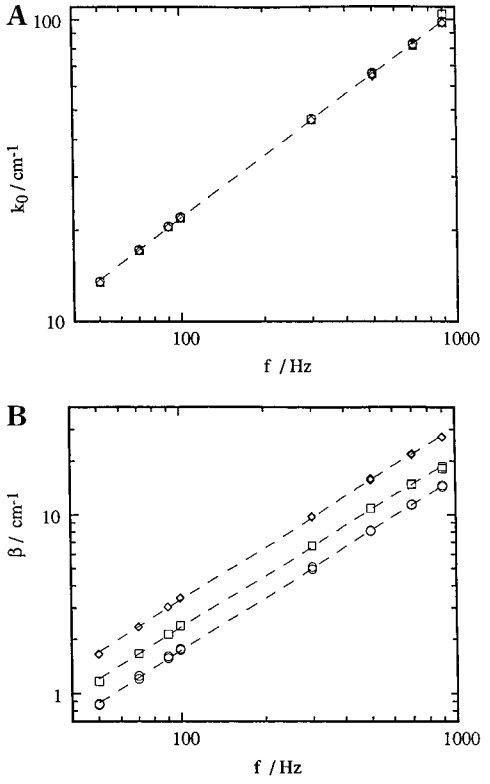

Figure 6. (A) Wave vector as a function of frequency for the air/PEG system at (◇) 40 °C, (□) 55 °C, and (○) 70 °C. The slope of the dashed line is 0.68. (B) Damping constant as a function of frequency for the air/PEG system at the same three temperatures as in panel A.

frequency difference over the range examined. Summarized in Table 3 are the temperature dependences. A value of −0.093 ± 0.005 (mN/m)/K was obtained for the surface tension temperature coefficient. This is in good agreement with the literature value of −0.098 (mN/m)/K.[30] Here, the molecular weight dependence of PEG is known to be slight because of the chain end hydrogen bonding, resulting in effective high molecular weight of oligomers in bulk.[5]

As with PDMS, we see from Tables 2 and 3 that the viscosities obtained by the ECWD technique are in good agreement with those by the conventional techniques, though agreement is not as good for the surface tension. The difference is still less than 7%. Double-logarithmic plots of wave vector and damping constant as a function of frequency are displayed in Figure 6. When the frequency is below 1 kHz, PEG also follows the Stokes limiting behavior, which means that the viscosity effect is small for this PEG sample. At 25 °C and high frequency range (>1.5 kHz), PDMS and PEG show different behaviors. For PDMS, at 2 kHz, reproducible data could be obtained though its standard deviation becomes larger than those at low frequencies (<1 kHz). For PEG, the linearities of phase and amplitude vs the radial distance at high frequency were not well established even in a very short distance. Hence the errors became quite large. It is possible that this comes about by the appearance of bulk overdamped mode. Dispersion eq 4, can be parametrized in the form:[26]

$$4Q^4 + (1/P)Q^3 - 4\,\mathrm{i}\,Q^2 - 1 = 4Q^{3+}\sqrt{(Q^2 - \mathrm{i})} \quad (9)$$

where + denotes the square root whose real part is positive and

$$Q \equiv k_o/(\omega\rho/\eta)^{1/2} \tag{10}$$

and

$$P \equiv (\omega\eta^3/\rho\sigma^2)^{1/2} \tag{11}$$

Solving for eq 11, one finds that there exist two different modes depending on P values, i.e., one is a viscous damped mode and the other is an overdamped solution (see Figure 1 of ref 26). The second overdamped mode does not appear if $P < P_{\text{critical}}$ ($\simeq$0.105). This mode is not a surface wave in the sense that the wave progagates into the fluids rather than being localized near the surface. For PDMS at $T = 40$ °C and high frequency of $\omega = 2000$ rad·s^{-1}, $\rho = 0.915$ g/cm^3, $\sigma = 18.7$ dyn/cm, $\eta = 0.1$ poise, and P is about 0.079, which is below the P_{critical} value. Hence the overdamped mode does not appear in the PDMS wave mode. For PEG at $T = 40$ °C and high frequency of $\omega = 2000$ rad·s^{-1}, $\rho = 1.078$ g/cm^3, $\sigma = 39.88$ dyn/cm, $\eta = 0.205$ poise, and $P \simeq 0.098$, which is quite close to the P_{critical} value. At $T = 25$ °C and 1 kHz, the P value for PDMS is 0.051 but 0.16 for PEG which is far above P_{critical}, and the overdamped mode should appear. This is a slowly damped and long wavelength mode, and this mode affects the wave behavior at long distance. Deviation from the linearities between the phase and amplitude vs the radial distance occurs more prominently from PEG at low temperature because the effect of fluid viscosity is more important than those due to surface tension changes. As the viscosity of the fluid increases (and so the effective molecular weight), a new mode called elastic mode appears. Recently, this was theoretically investigated by Harden et al. for concentrated polymer solutions.[31] Others experimentally tried to prove the mode transition from the capillary to elastic mode with the concentration of the solution, but the issue merits further examination in conjunction with careful viscoelastic measurements.[32,33]

Summary

We have determined the surface tensions and viscosities through the capillary wave dispersion relation for oligomers of PDMS and PEG at three different temperatures in a narrow range of 40−70 °C. Good agreement of surface tension values with the literature values shows that the ECWD technique can be used for this purpose for relatively high viscous medium compared to water. Temperature gradient of the surface tension, dγ/dT, of PEG agrees well with the literature despite its low molecular weight, presumably due to its end group hydrogen bonding, whereas that of PDMS shows a small difference from that of its polymers due to its low molecular weight. The behaviors of PDMS and PEG are different at high frequencies, especially at a low temperature, due to the appearance of the overdamped mode. Deviation from the linearities happens at a shorter distance from the source point for PEG than PDMS due to the second mode.

PDMS shows an interesting phenomenon of the presence of surface waves with the same frequency as the applied voltage. We believe this happened because of its helical structure. However capillary wave properties are unaffected by the appearance of the 1f mode.

This study shows that ECWD can be used to determine the surface properties of bulk fluids of which the viscosity is relatively higher than that of water. It can be used to analyze the monolayer film properties floated on a viscous medium which would show a different behavior from those on water. This is currently under investigation and will be published in a forthcoming paper.

Acknowledgment. This is in part supported by the polymers program of NSF (DMR-9203289), Eastman Kodak Co., and the Helfaer Professorship of the University of Wisconsin to H.Y. Also, Y.S. is indebted to the exchange program of the Korea Institute of Science and Technology (No. 2E14024) for the opportunity to visit the University of Wisconsin in 1994 and 1996.

References and Notes

(1) Irja, P. *Polymeric Surfactants*; Marcel Dekker Inc.: New York, 1992.
(2) Myers, D. *Surfaces, Interfaces,* and *Colloids*; VCH Publishers: New York, 1991.
(3) Feast, W. J., Munro, H. S., Richards, R. W., Eds. *Polymer Surfaces and Interfaces (II)*; Wiley: Chichester, England, 1993.
(4) Garbassi, F.; Morra, M.; Orchello, E. *Polymer Surfaces*; Wiley: Chichester, England, 1994.
(5) Wu, S. *Polymer Interface and Adhesion*; Marcel Dekker: New York, 1982.
(6) Langevin, D., Ed. *Light Scattering by Liquid Surfaces*; Marcel Dekker: New York, 1991.
(7) Sauer, B. B.; Kawaguchi, M.; Yu, H. *Macromolecules* **1987**, *20*, 2732.
(8) Stanley, H. E. *Introduction to Phase Transitions and Critical Phenomena*; Oxford University Press: New York, 1971; p 228.
(9) Kohler, F. *The Liquid State*; Verlag Chemie: Weinheim, 1972; Chapter 9.
(10) Chu, B. *Laser Light Scattering*, 2nd ed.; Academic Press: New York, 1991; p 45.
(11) Langevin, D. *Prog. Colloid Polym. Sci.* **1990**, *83*, 10.
(12) Runge, F.; Yu, H. *Langmuir* **1993**, *9*, 3191. Runge, F.; Kent, M. S.; Yu, H. *Langmuir* **1994**, *10*, 962.
(13) Kawaguchi, M.; Sano, M.; Chen, Y. L.; Zografi, G.; Yu, H. *Macromolecules* **1986**, *19*, 2606.
(14) Yoo, K. H.; Yu, H. *Macromolecules* **1989**, *22*, 4019.
(15) Gau, C. S.; Yu, H.; Zografi, G. *Macromolecules* **1993**, *26*, 2524. Gau, C. S.; Yu, H.; Zografi, G. *J. Colloid Interface Sci.* **1994**, *162*, 214.
(16) Ito, K.; Sauer, B. B.; Skarlupka, R. J.; Sano, M.; Yu, H. *Langmuir* **1990**, *6*, 1379.
(17) Lemaire, C.; Langevin, D. *Colloids Surf.* **1992**, *65*, 101.
(18) Lee, K. Y.; Chou, T.; Chung, D. S.; Mazur, E. *J. Phys. Chem.* **1993**, *97*, 12876.
(19) Abramowitz, M.; Stegun, I. A. *Handbook Mathematical Functions*; Dover: New York, 1972.
(20) Skarlupka, R. J. Ph.D. Dissertation, University of Wisconsin−Madison, 1990.
(21) Jiang, Q.; Chiew, Y. C. *Langmuir* **1992**, *8*, 2747.
(22) Stenvot, C.; Langevin, D. *Langmuir* **1988**, *4*, 1179.
(23) Lucassen-Reynders, E. H.; Lucassen, J. *Adv. Colloid Interface Sci.* **1969**, *2*, 347.
(24) LeGrand, D. G.; Gaines, G. L., Jr. *J. Polym. Sci. Part C* **1971**, *34*, 44.
(25) Ferry, J. D. *Viscoelastic Properties of Polymers*; Wiley: New York, 1980; Chapter 11.
(26) Sohl, C. H.; Miyano, K. *Phys. Rev. A* **1979**, *20*, 616.
(27) Mark, J. E.; Allcock, H. R.; West, R. *Inorganic Polymers*; Prentice-Hall: Englewood Cliffs, NJ, 1992; Chapter 2.
(28) Runge, F.; Stauffer, H. U.; Lenk, T. J.; Koberstein, J. T.; Yu, H. *Langmuir*, in press.
(29) Jackson, J. D. *Classical Electrodynamics*; Wiley: New York, 1962.
(30) Brandrup, I., Immergut, E. H., Eds. *Polymer Handbook*; Wiley: New York, 1989.
(31) Harden, J. L.; Pleiner, H.; Pincus, P. A. *Langmuir* **1989**, *5*, 1436; *J. Chem. Phys.* **1991**, *94*, 5208.
(32) Cao, B. H.; Kim, M. W.; Chaffer, H.; Cummins, H. Z. *J. Chem. Phys.* **1991**, *95*, 9317.
(33) Dorshow, R. B.; Turkevich, L. A. *Phys. Rev. Lett.* **1993**, *70*, 2439.

MA961095L